

# Reconstruction of 3D Patient-Specific Bone Models From Biplanar X-Ray Images Utilizing Morphometric Measurements

Mohamed Mahfouz , Ahmed Badawi, Emam E. Abdel Fatah, Michael Kuhn, Brandon Merkl

Biomedical Engineering Department, University of Tennessee Knoxville

*Abstract - Obtaining 3D patient-specific bone models from 2D image data (e.g. X-rays, fluoroscope) remains a practical and desirable alternative to segmentation of bone models from 3D image data (e.g. CT, MRI). It also provides an initial step to automatically calculating the relevant axes and angles needed in computer aided surgery (CAS). Our method utilizes a statistical atlas of bone based on Principal Component Analysis (PCA) and biplanar X-ray images to fully reconstruct a patient-specific 3D bone model. Reconstruction is done through a robust 3D-2D registration technique where the deformation is constrained through extracted 2D morphometric measurements. Reconstructions of both femur and lumbar were undertaken with results compared to manual segmentations.*

**Keywords: 3D Reconstruction, Bone, Biplanar X-Ray, Morphometry**

## 1. Introduction

The use and far reaching potential for different types of surgical navigation systems, especially in the area of Computer Aided Surgery (CAS), has begun to be realized with the increasing prevalence of high technology equipment and advanced 3D graphics systems in the medical field. The new tools available to surgeons through the use of CAS in both preoperative and intraoperative steps are bringing unprecedented accuracy and reliability to the orthopedic industry [1]. A fundamental part of any CAS system during surgery is registering 3D patient-specific bone models to *in vivo* data real-time. Only after accurately registering the patient-specific bone models to *in vivo* data, a full 3D analysis of the joint can be undertaken.

One preoperative step that must be performed is constructing the relevant patient-specific 3D bone models. The obvious method for this step is to have the patient CT scanned and then manually segment 3D surface models from the volumetric data. Although this method is proven to work well, the high cost combined with the large dose of radiation leads to seeking lower

cost alternatives. One method that has been extensively researched is reconstructing 3D bone models from biplanar X-ray images. Many of these 3D-2D registration techniques have focused on landmark detection. Manually picking landmarks can provide accurate results in certain cases, but is too simplistic an approach for most applications [2] as it can be sensitive to noise and the shape of the contour, especially in applications like the spine [3].

An obvious solution to this problem is incorporating active shape models and active appearance models [4]. Much of the work in this area, though, has focused on simplified shape models that only incorporate major landmarks or other prominent features on the bone [5]. In our method, a robust statistical atlas of bone is incorporated into the biplanar reconstruction. The bone atlas, combined with a powerful 3D-2D registration algorithm [6] constrained with automated morphometric and surgical measurements provide the framework needed for accurate results to this difficult problem.

## 2. Materials and Methods

### 2.1 Overview

The process our method follows is outlined in Figure 1. Automated morphometric and surgical axis measurements are performed on the biplanar images to estimate the shape and the size of the bone which helps increase the speed and accuracy of the registration process. The average bone from the atlas is placed in a 3D scene with two or more X-ray images as in Figure 2, and the user provides an initial pose for the 3D rigid alignment. The average bone and initial pose are used to create a normally distributed initial population of bone models (represented in the atlas) centered around the average bone at the initial pose. The shape parameters, translation, and rotation combine for a 12+ DOF optimization problem. The genetic algorithm is then used, along with our novel 3D-2D scoring metric and the previous calculated measurements, to optimize both the shape and alignment of the population to the X-ray images.

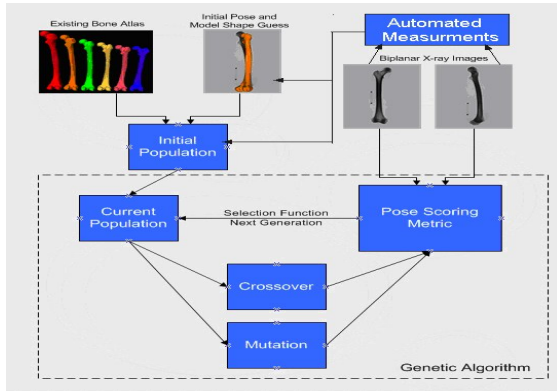


Figure 1: Outlined biplanar reconstruction process

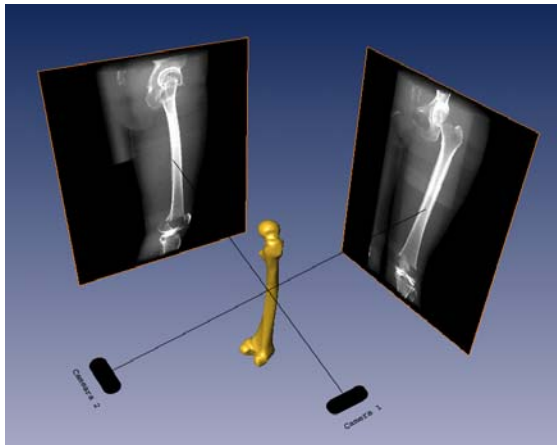


Figure 2: 3D visualization of virtual biplanar scene

## 2.2 Automated Measurements

This includes a combination of both morphometric and surgical measurements that differ from one bone to another. Measurements are carried out first on the biplanar images in order to get an estimate of both size and shape of the bone that can be used later with the registration process to constrain the search space of the genetic algorithm. The first step involves automatic detection of bone landmarks through a combination of advanced pattern recognition, mathematical, and geometrical techniques. For the femur, five morphometric measurements are carried out. Figure 3 outlines the measurements where “A-B” is the maximum length, “C-D” is the bicondylar (oblique or physiological) length, “S-T” is the anteroposterior diameter of the midshaft, and “M-N” is the mediolateral diameter of the midshaft. Figure 4 shows some of the automated surgical axes (e.g. anatomical axis, mechanical axis, transepicondylar axis, femoral axis, and posterior condylar axis).

## 2.3 Genetic Algorithm

Genetic algorithms represent a class of complex global optimization techniques that mimic the process of

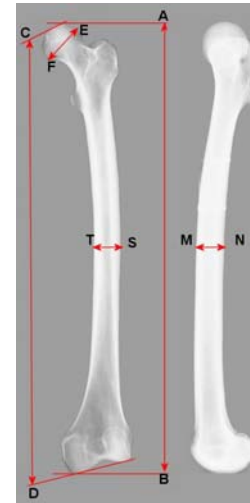


Figure 3: Femur morphological measurements



Figure 4: Automated surgical measurements on femur

natural selection. First a randomized population of individuals is created, where each individual represents a particular instance to a solution of the problem. Each member of the population is scored (or ranked) using an objective function that measures the ability of an individual to solve the problem at hand. After the initial population is generated, individuals, stochastically selected by their larger scores, are chosen to reproduce, usually in a crossover or mutation mechanism. Since the genetic algorithm is relatively insensitive to local minima, and has been used for other complex surface generation problems [7], we have found it to be quite suitable for this application.

## 2.4 DRR Generation

Digitally reconstructed radiographs (DRRs) are synthetic x-rays generated by casting rays according to specific camera geometry through the CT volume [8]. We created the DRRs using a novel volume rendering technique which closely follows the attenuation observed in X-ray images through different media (bone, soft tissue, fat, muscle, etc.). Figure 5 shows a

sample set of orthogonal DRRs generated from a cadaver CT dataset.



Figure 5: Biplanar DRRs for a cadaver leg

## 2.5 Biplanar 3D/2D Registration

The algorithm to register the bone of interest to both images is posed as an optimization problem of both predicted model shape and orientation. The objective function consists of the sum of a matching metric calculated for each image. Thus the objective function is the combination of matching scores computed for individual images. To compute the matching score for each image, a hypothesized pose and shape of the bone model are projected onto the virtual image plane for each image. The predicted 2D image is matched to each of the X-ray images using the robust method proposed by Mahfouz et al. [6].

Highlights of the method include incorporating region and edge scoring metrics into the overall matching score. The 2D projection of the bone model is separated into two images: the region image is binary with all pixels in the silhouette of the model white, the edge image incorporates Prewitt edge detection on the silhouette and spreading of the resulting edge using a Gaussian smoothing filter. A complete explanation can be found in [6].

The initial alignment provided by the user is used to constrain the bounds of translation and rotation during optimization. An initial optimization is run in which only the translation and rotation of the base model are allowed to vary. This allows higher constraints when varying both the shape parameters and position/orientation. This first optimization problem is only 6 DOF while the final bone morphing one can be 10-15 DOF.

When the genetic algorithm has converged to a rigid alignment, the best member of the population is used as a genetic dopant in a second optimization step. The second genetic algorithm operates on the same objective function as the first, but now is given additional DOF associated with shape parameters of the statistical atlas. Depending on bone type, the shape parameters for the statistical atlas range from 3 principal components (PCs) capturing 99.5% of the variation for full femurs, to 5 PCs which capture a similar percentage of cumulative variation in L5

vertebrae. In this 2<sup>nd</sup> run, the genetic algorithm still optimizes the 6 DOF for rigid alignment, but also adds the prominent shape parameters as more DOF. The 1<sup>st</sup> optimization allows the 2<sup>nd</sup> to be further constrained, so that the search space of this high DOF problem can be reduced.

## 2.6 Algorithm Verification

In testing this algorithm we have tried two synthetic methods. First, using an atlas of L5 lumbar vertebrae we have generated silhouette-like grayscale images that contain image noise. In this test we generated the images using a random perturbation of the shape parameters with the model in an arbitrary pose. We added Gaussian noise to both the rigid pose parameters and the shape parameters for 20 runs and measured 14 instances of convergence among the models. Here we know both the exact pose and the exact shape of the bone model, which would not be the case for actual patient data. This method, though synthetic, provides a framework for analyzing the range of convergence and the overall accuracy of the algorithm under idealized conditions. Since we know everything about the true pose and the true shape, we can measure the RMS error of the pose and shape parameters.

A second method of verification performed was running the biplanar 3D/2D matching algorithm on DRRs generated from a full femur using our previously discuss method. In this experiment we generated DRRs for the full femur for anterior/posterior and lateral views. We had previously segmented the femur from the original CT dataset used to generate the DRRs, so the true shape is known. Figure 6 shows the initial pose of the mean femur for A/P and lateral views.



Figure 6: Biplanar DRR initial poses

Table 1: RMS error, R values are fixed XYZ Euler angles in radians, T represents translation in mm

Rigid parameter	$R_x$	$R_y$	$R_z$	$T_x$	$T_y$	$T_z$
	0.06	0.01	0.05	0.52	0.24	1.8

Table 2: RMS error for first five shape parameters, unitless

Shape parameter	$PC_1$	$PC_2$	$PC_3$	$PC_4$	$PC_5$
Mean RMS	0.07	0.05	0.15	0.05	0.03

### 3. Results

RMS error for the rigid pose and shape parameters for the lumbar experiment are shown in Tables 1 and Table 2. We also measured the point-to-point surface errors between the known model and the reconstructed model and found that the average point-to-surface RMS error was 0.132 mm (for the lumbar), with the best pose found shown in Figure 7. Figure 8 has a point-to-surface RMS error of 0.033 mm. Figure 9 shows the point-to-point surface mapping between the true model and the reconstructed model for the full femur.

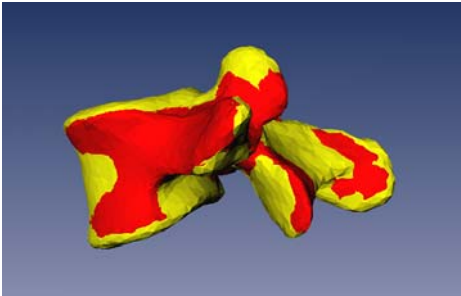


Figure 7: Best overall pose for L5 vertebra (dark model is true pose, light model is reconstructed)

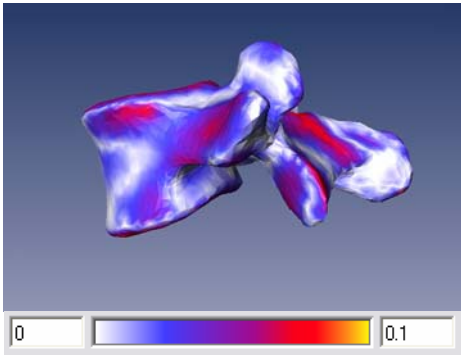


Figure 8: Best overall pose found for L5 lumbar vertebrae visualized as a distance map of surface error on the reconstructed model (light color represents 0.0 mm error, darker color is 0.1 mm)

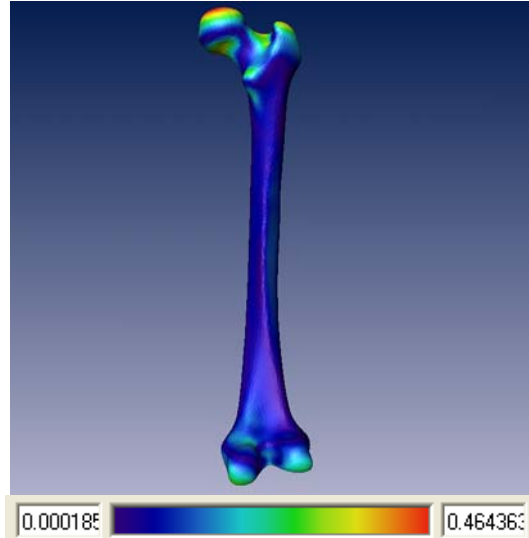


Figure 9: Best overall pose found for femur visualized as a distance map of surface error on the reconstructed model (blue colour represents 0.000185 mm error, darker colour is 0.464 mm)

### 4. Conclusions

Preliminary results indicate that our method can reconstruct lumbar vertebrae to produce accurate contour projections from orthogonal views. Specifically, we have shown how using a complex optimization algorithm combined with image processing methods can yield reasonable results. We have also tested our algorithm using synthetically generated DRRs that take into account actual variation of X-ray absorption in tissues such as muscle, fat, bone, and skin. Since the DRRs contain image noise from the original CT, the resultant image mimics the real-world environment in which actual patient X-rays would be taken. We wish to further our investigation to incorporating actual patient X-rays and a coherent calibration system [9,10] to extract both the intrinsic and extrinsic camera parameters.

The biplanar method has the potential to construct even more difficult bones such as the cranium or sacrum when combined with a statistical atlas and multiple views. Since each additional view helps to resolve out-of-plane registration errors associated with one perspective, we remain optimistic that our algorithm can tackle even more difficult problems. Additionally, the biplanar method is attractive because if a view has partial occlusion, it is unlikely its orthogonal counterpart also will.

## 5. References

- [1] SIMON D., LAVALLEE S. "Medical Imaging and Registration in Computer Assisted Surgery", *Clin. Ortho. & Rel. Research*, 354: 17-27, 1998.
- [2] MITULESCU A., SEMAAN I., DE GUISE J., LEBORGNE P., ADAMSBAUM C., SKALLI W. "Validation of the nonstereo corresponding points stereoradiographic 3-D reconstruction technique", *Med. Biol. Eng. Comput.*, 39: 152-158, 2001.
- [3] ANDRE B., DANSEREAU J., LABELLE H. "Optimized vertical stereo base radiographic setup for the clinical three-dimensional reconstruction of the human spine", *J Biomechanics*, 27(8): 1023-1025, 1994.
- [4] BENAMEUR S., MIGNOTTE M., PARENT S., LABELLE H., SKALLI W., DE GUISE J. "3D/2D registration and segmentation of scoliotic vertebrae using statistical models", *Computerized Med. Imag. and Graph.*, 27: 321-337, 2003.
- [5] KAUFFMANN B., GODBOUT B., DE GUISE J. "Simplified active contour model applied to bone structure segmentation in digital radiographs", *Proc. SPIE*, 3338: 663-672, 1998.
- [6] MAHFOUZ M., HOFF W., KOMISTEK R., DENNIS D. "A Robust Method for Registration of Three-Dimensional Knee Implant Models to Two-Dimensional Fluoroscopy Images", *Med. Imag., IEEE Trans.*, 22(12): 1561-1574, 2003.
- [7] TOHKA J. "Global Optimization of Deformable Surface Meshes Based on Genetic Algorithms", *Proc. 11<sup>th</sup> Int. Conf. on Img. Anal. and Proc.*, Palermo, Italy: 459 – 464, 2001.
- [8] RUSSAKOFF D., ROHLFING T., RUECKERT D., SHAHIDI R., KIM D., MAURER C. "Fast calculation of digitally reconstructed radiographs using light fields", *Proc. SPIE*, 5032: 684-695, 2003.
- [9] CHERIET F., MEUNIER J. "Self-calibration of a biplane X-ray imaging system for an optimal three dimensional reconstruction", *J Comput Med Imag Graph*, 23(3): 133-141, 1999.
- [10] DUMAS R., MITTON D., LAPORTE S., DUBOUSSET J., STEIB J., LAVASTE F., SKALLI W. "Explicit calibration method and specific device designed for stereoradiography", *J Biomechanics*, 36(6): 827-834, 2003.